

# Reaction of Ru<sub>3</sub>(CO)<sub>12</sub> with Dibenzylideneacetone

Svetlana V. Osintseva, Fedor M. Dolgushin,\* Nikolay A. Shtel'tser,  
Pavel V. Petrovskii, Arkadii Z. Kreindlin, Leonid V. Rybin,† and  
Mikhail Yu. Antipin

A.N. Nesmeyanov Institute of Organoelement Compounds, Russian Academy of Sciences,  
28 Vavilov Street, 119991 Moscow, Russian Federation

Received December 17, 2004

The thermal reaction of Ru<sub>3</sub>(CO)<sub>12</sub> with dibenzylideneacetone PhCH=CHCOCH=CHPh (**1**) was studied. From the solution, the trinuclear complexes Ru<sub>3</sub>(CO)<sub>6</sub>{μ<sub>3</sub>-η<sup>2</sup>-η<sup>2</sup>-η<sup>2</sup>-O=C(CH=CHPh)-CH=CPh}<sub>2</sub> (**6**) and Ru<sub>3</sub>(CO)<sub>7</sub>{η<sup>2</sup>-O=C(CH=CHPh)CH=CPh}{μ-η-η<sup>4</sup>-O-C(CH=CHPh)-CH-CPh-CH(CH<sub>2</sub>Ph)C(O)(CH=CHPh)}{μ<sub>3</sub>-η-η-η<sup>4</sup>-(CH<sub>2</sub>Ph)CH=C(O)-CH=CHPh} (**7**) were isolated, and the precipitate was found to contain the tetranuclear complex Ru<sub>4</sub>(CO)<sub>8</sub>{μ<sub>3</sub>-η-η<sup>2</sup>-η<sup>6</sup>-O-C(CH=CHPh)=CH-CPh-CH(CH<sub>2</sub>Ph)-C(O)-CH=CHPh}<sub>2</sub> (**8**). The organic ligand in complexes realizes different coordination modes forming five-membered oxaruthenacycle, η<sup>3</sup>-coordinated dihydropyran cycle, η<sup>4</sup>-coordinated diene, or oxadiene fragments. Complex **7** is unstable and undergoes chemical transformations yielding complex **8**. Reversible changes occur with complex **8** upon dissolution in acetone, and binuclear complex Ru<sub>2</sub>(CO)<sub>4</sub>(η-O=CMe<sub>2</sub>)(μ-η-η<sup>2</sup>-η<sup>6</sup>-O-C(CH=CHPh)=CH-CPh-CH(CH<sub>2</sub>Ph)-C(O)-CH=CHPh) (**9**) is formed. The central Ru<sub>2</sub>O<sub>2</sub> cycle in complex **8** is cleaved and the formed vacant coordination site is occupied by an acetone molecule in complex **9**. Complexes **6–9** were characterized by IR and <sup>1</sup>H NMR spectroscopy, and their structures were determined by single-crystal X-ray diffraction analysis. The structural and spectroscopic features and possible pathways of the complexes' transformations are discussed.

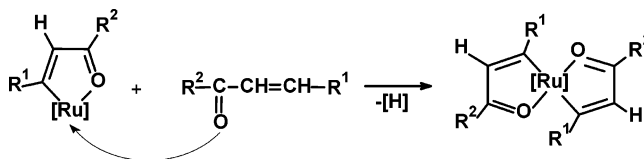
## Introduction

Transition metal complexes of α,β-unsaturated ketones are important intermediates in the synthesis of organic products such as β-lactams,<sup>1a,b</sup> amino acids,<sup>1c</sup> phenols,<sup>1d</sup> and heterocyclic compounds.<sup>1e</sup> However, reports on the coordination chemistry of these ligands with transition metals are scarce, although the presence of the C=O ketone and C=C double bond in these molecules may lead to a wide reactivity and various coordination patterns.

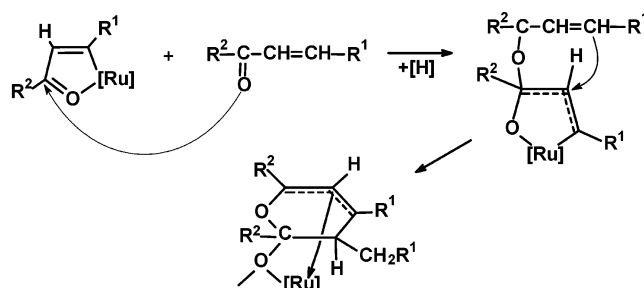
Over the past decade, we have conducted systematic studies on the reactivity of the α,β-unsaturated ketones in thermal reactions with ruthenium carbonyls.<sup>2a–d</sup> Thermally activated reactions of Ru<sub>3</sub>(CO)<sub>12</sub> with 4-phenylbut-3-en-2-one (**1a**),<sup>2a,b</sup> 3-phenyl-1-*p*-tolylprop-2-en-1-one (**1b**),<sup>2a,b</sup> or 1,3-diferrocenylprop-2-en-1-one (**1c**)<sup>2c,d</sup> yield, as primary products, bi- and trinuclear complexes of ruthenium containing one or two η<sup>3</sup>-coordinated five-membered oxaruthenacycles, i.e., Ru<sub>2</sub>(CO)<sub>6</sub>(μ-H)(R<sup>1</sup>C=C(H)C(O)R<sup>2</sup>) (**2**) and Ru<sub>3</sub>(CO)<sub>8</sub>(R<sup>1</sup>C=C(H)C(O)R<sup>2</sup>)<sub>2</sub> (**3**) (Scheme 1). These five-membered chelate oxaruthenacycles are formed via oxidative addition of a ruthenium atom to the C<sub>β</sub>-H bond with simultaneous coordination of the keto-oxygen electron lone pair. Further, acting as ligand, the oxaruthenacycle can form η<sup>3</sup>-complexes through the C=C bond and the Ru atom.

Reactivity of these oxaruthenacycles in further reaction with the initial α,β-unsaturated ketone is defined

by the two electron-deficient centers, viz., the ruthenium atom and the carbon atom of the former keto group. The attack by the nucleophilic center of the α,β-unsaturated ketone (i.e., by the keto-oxygen atom) proceeds competitively at these two sites.<sup>2d</sup> In the former case, addition to the ruthenium atom is followed by ligand chelation, which results in the closing of the second oxaruthenacycle, yielding complex **4**.

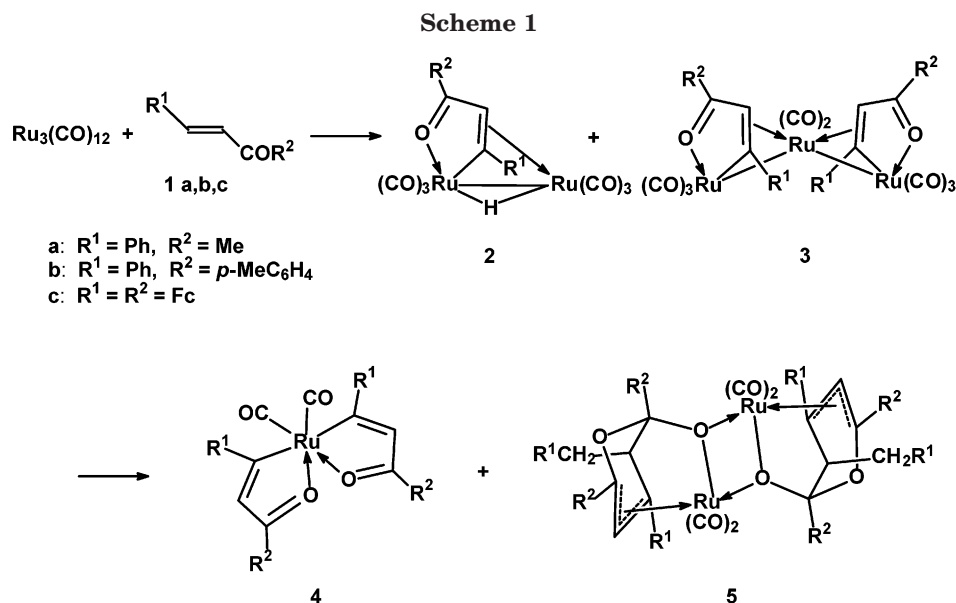


In the latter case, addition to the carbon atom of the oxaruthenacycle carbonyl group gives rise to the dihydropyran ring, which gets involved in the coordination to other ruthenium atoms through the multiple C=C bonds and the lone pair of the exocyclic oxygen atom (complex **5**).



\* Corresponding author. E-mail: fedya@xrlab.ineos.ac.ru.

† Prof. Leonid V. Rybin died in 2003.



Minor products of these reactions mainly present species containing combinations of the same cyclic fragments, i.e., oxaruthenacycles and dihydropyran rings.

In addition, we have studied thermal reactions of  $\text{Ru}_3(\text{CO})_{12}$  with dibenzoyl ethylene ( $\text{PhCOCH}=\text{CHCOPh}$ )<sup>2e</sup> and dimethyl fumarate ( $\text{CH}_3\text{OOCCH}=\text{CHCOOCH}_3$ ).<sup>2f</sup> The main structural block of the complexes thus obtained was still the oxaruthenacycle. However, the presence of additional centers available for coordination, i.e., oxygen lone pairs, leads to bicyclic systems, in which both oxygen atoms are involved in the chelation of two different ruthenium atoms.

In the present paper, we report on the reactivity of dibenzylideneacetone (DBA),  $\text{PhCH}=\text{CHCOCH}=\text{CHPh}$  (**1**), in the thermally activated reaction with  $\text{Ru}_3(\text{CO})_{12}$ . In contrast to all earlier studied  $\alpha,\beta$ -unsaturated ketones, DBA contains two symmetric olefin groups, which allows additional possibilities for coordination to metal atoms. In this respect a formation of complexes with earlier unobserved coordination modes may be suggested. Furthermore, the interest in the DBA ligand is due to its role in organometallic chemistry. In particular, palladium DBA complexes have been extensively used

in ligand exchange reactions.<sup>3a-c</sup> Numerous palladium complexes containing DBA, along with other ligands such as phosphines, isocyanates, amines, olefins, and acetylenes, have been prepared and characterized.<sup>3d-i</sup> Extension of synthetic methods developed for palladium to other metals led to development of DBA complexes of Pt,<sup>4</sup> Rh,<sup>5a</sup> and Ir.<sup>5b</sup> In the Pt, Pd, Rh, and Ir complexes known so far, the DBA ligand is most frequently  $\pi$ -coordinated through one of the C=C bonds or, less frequently, through both C=C bonds; coordination through the oxygen atom or C=O double bond has never been observed.

A number of complexes have been synthesized not directly from DBA or substituted divinylideneacetones, but rather as a result of coupling of acetylenes coordinated to transition metal clusters with participation of metal-coordinated carbonyls. Such reactions have been realized for Mo<sup>6a</sup> and Mn,<sup>6b,c</sup> and no  $\pi$ -coordination was observed in these complexes.

Complexes of metals from the iron subgroup with the DBA ligand,<sup>7a,b</sup> involving a variety of substituted divinylideneacetones<sup>7c,d</sup> and ligands, produced via coordination-assisted coupling of acetylenes and carbonyl ligand,<sup>7e,f,g</sup> manifest the most diverse coordination modes. The ligand binding therein may be realized either

(1) (a) Howell, J. A. S. *Chemistry of Enones*; Patai, S., Rappoport, Z., Eds.; John Wiley & Sons Ltd.: New York, 1989. (b) Hegedus, L. S.; Imwinkelreid, R.; Alarid-Sargent, M.; Drorak, D.; Saton, Y. *J. Am. Chem. Soc.* **1990**, *112*, 1109. (c) Hegedus, L. S.; Schwindt, M. A.; Delombert, S.; Imwinkelreid, R. *J. Am. Chem. Soc.* **1990**, *112*, 2264. (d) Morris, G.; Saberi, S. P.; Thomas, S. E. *J. Chem. Soc., Chem. Commun.* **1993**, 209. (e) Dosreis, A. C.; Hegedus, L. S. *Organometallics* **1995**, *14*, 1586.

(2) (a) Rybinskaya, M. I.; Rybin, L. V.; Osintseva, S. V.; Dolgushin, F. M.; Yanovsky, A. I.; Struchkov, Yu. T. *Russ. Chem. Bull.* **1995**, *44*, 154 [*Izv. Akad. Nauk, Ser. Khim.* **1995**, 159]. (b) Rybin, L. V.; Osintseva, S. V.; Batsanov, A. S.; Struchkov, Yu. T.; Petrovskii, P. V.; Rybinskaya, M. I. *Russ. Chem. Bull.* **1993**, *42*, 1228 [*Izv. Akad. Nauk, Ser. Khim.* **1993**, 1285]. (c) Rybin, L. V.; Osintseva, S. V.; Petrovskaya, E. A.; Kreindlin, A. Z.; Dolgushin, F. M.; Yanovsky, A. I.; Petrovskii, P. V.; Rybinskaya, M. I. *Russ. Chem. Bull.* **2000**, *44*, 154 [*Izv. Akad. Nauk, Ser. Khim.* **2000**, 1616]. (d) Osintseva, S. V.; Dolgushin, F. M.; Petrovskii, P. V.; Shteltser, N. A.; Kreindlin, A. Z.; Rybin, L. V.; Rybinskaya, M. I. *Russ. Chem. Bull.* **2002**, *51*, 1754 [*Izv. Akad. Nauk, Ser. Khim.* **2002**, 1610]. (e) Rybinskaya, M. I.; Rybin, L. V.; Osintseva, S. V.; Dolgushin, F. M.; Yanovsky, A. I.; Struchkov, Yu. T.; Petrovskii, P. V. *J. Organomet. Chem.* **1997**, *536-537*, 345. (f) Shteltser, N. A.; Rybin, L. V.; Petrovskaya, E. A.; Batsanov, A. S.; Djafarov, M. X.; Struchkov, Yu. T.; Rybinskaya, M. I.; Petrovskii, P. V. *Organomet. Chem. USSR* **1992**, *4* [*Metalloorg. Khim.* **1992**, *5*, 1009].

(3) (a) Ukai, T.; Ishii, H.; Bonnet, J. J.; Ibers, J. A. *J. Organomet. Chem.* **1974**, *65*, 253. (b) Mazza, M. C.; Pierpont, C. G. *Inorg. Chem.* **1973**, 2955. (c) Tsuji, T. *Palladium Reagents and Catalysts: Innovations in Organic Synthesis*; Wiley: Chichester, 1995. (d) Amatore, C.; Jutand, A. *Coord. Chem. Rev.* **1998**, *178-180*, 511. (e) Pierpont, C. G.; Buchanan, R. M.; Downs, H. H. *J. Organomet. Chem.* **1977**, *124*, 103. (f) Herrmann, W. A.; Thiel, W. R.; Brossmer, C.; Ofefe, K.; Priermeier, T.; Scherer, W. *J. Organomet. Chem.* **1993**, *461*, 51. (g) Burrows, A. D.; Choi, N.; McPartlin, M.; Mingos, D. M. P.; Tarlton, S. V.; Vilar, R. *J. Organomet. Chem.* **1999**, *573*, 313. (h) Selvakumar, R.; Valentini, M.; Worle, M.; Pregosin, P. S.; Albinati, A. *Organometallics* **1999**, *18*, 1207. (i) Reid, S. M.; Mague, J. T.; Fink, M. J. *J. Organomet. Chem.* **2000**, *616*, 10.

(4) (a) Lewis, L. N.; Krafft, T. A.; Huffman, J. C. *Inorg. Chem.* **1992**, *3555*. (b) Fong, S. W. A.; Vittal, J. J.; Hor, T. S. A. *Organometallics* **2000**, *19*, 918.

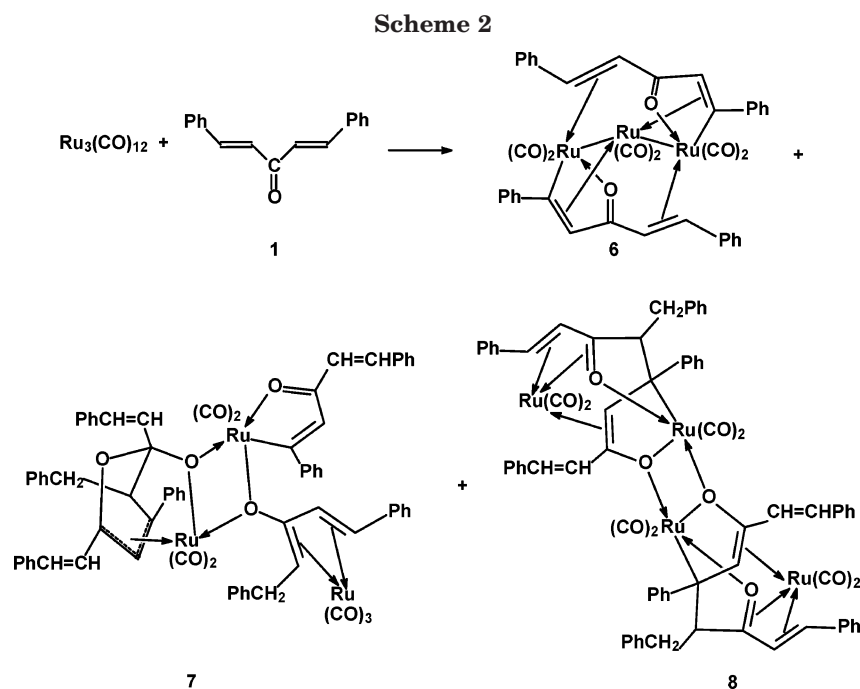
(5) (a) Ibers, J. A. *J. Organomet. Chem.* **1974**, *73*, 389. (b) Orpen, A. G.; Pringle, P. G.; Smith, M. B.; Worboys, K. *J. Organomet. Chem.* **1998**, *550*, 255.

(6) (a) Allen, S. A.; Green, M.; Norman, N. C.; Paddick, K. E.; Orpen, A. G. *J. Chem. Soc., Dalton Trans.* **1983**, 1625. (b) Adams, R. D.; Chen, L.; Wu, W. *Organometallics* **1993**, *12*, 4112. (c) Adams, R. D.; Chen, G.; Chen, L.; Wu, W.; Yin, J. *Organometallics* **1993**, *12*, 3431.

Table 1. IR and NMR Spectra for Complexes 6–9

compound	IR $\nu(CO)$ , $cm^{-1}$	$^1H$ NMR $\delta$ , ppm ( $C_6D_6$ )
(PhCH=CH) $_2$ CO <sup>a</sup>	1668m, 1610s	7.08(d, 2H, CH=CH, $J = 16.0$ Hz), 7.35–7.62(m, 10H, Ph), 7.74(d, 2H, CH=CH, $J = 16.0$ Hz)
(PhCH $_2$ CH $_2$ ) $_2$ CO <sup>b</sup>	1684m, 1612s	2.27(t, 4H, CH $_2$ , $J = 7.8$ Hz), 2.94(t, 4H, CH $_2$ , $J = 7.8$ Hz), 7.30–7.70(m, 10H, Ph)
6 <sup>a</sup>	2046w, 2038s, 2028s, 1992m, 1978w, 1968w	4.36(d, 1H, CH=CH, $J = 12.8$ Hz), 4.65(d, 1H, CH=CH, $J = 12.8$ Hz), 5.35(s, 1H, CH=C), 7.18–7.98(m, 10H, Ph)
7 <sup>a</sup>	2056m, 2042s, 2016s, 1996m, 1980s, 1968m, 1938w	1.69–1.77(m, 2H, CH $_2$ ), 1.96(d, 1H, CH=CH, $J = 7.2$ Hz), 2.56–2.91(m, 3H, CH $_2$ -CH), 3.09–3.14(m, 1H, CH), 5.64(d, 1H, CH=CH, $J = 7.2$ Hz), 5.85(s, 1H, CH=C), 6.18(d, 1H, CH=CH, $J = 16.0$ Hz), 6.61–7.74(m, 44H, Ph, CH=CH, CH=C), 8.18(d, 1H, CH=CH, $J = 16.0$ Hz), 8.71(d, 1H, CH=CH, $J = 16.0$ Hz)
8 <sup>b</sup>	2034m, 2023s, 1964s, 1956s	2.66–2.91(m, 1H, CHH-CH), 3.67–3.70(m, 1H, CHH-CH), 4.15(d, 1H, CH=CH, $J = 8.8$ Hz), 4.46(s, 1H, CH=C), 5.42(m, 1H, CH $_2$ -CH), 6.36(d, 1H, CH=CH, $J = 8.8$ Hz), 6.89–7.57(m, 22H, Ph, CH=CH)
9 <sup>b,c</sup>	2027s, 2018s, 1939s, 1933s, 1701m	2.93(dd, 1H, $^2J_{H-H} = 15.6$ Hz, $^3J_{H-H} = 10.4$ Hz, CHH-CH), 3.38(dd, 1H, $^2J_{H-H} = 15.6$ Hz, $^3J_{H-H} = 2.8$ Hz, CHH-CH), 3.86(d, 1H, CH=CH, $J = 8.9$ Hz), 4.42(s, 1H, CH=C), 5.06(dd, 1H, $^3J_{H-H} = 10.4$ Hz, $^3J_{H-H} = 2.8$ Hz, CH $_2$ -CH), 6.14(d, 1H, CH=CH, $J = 8.9$ Hz), 7.1–7.65(m, 22H, Ph, CH=CH)

<sup>a</sup> IR in hexane. <sup>b</sup> IR in Nujol. <sup>c</sup>  $^1H$  NMR in acetone- $d_6$ , complex contains coordinated molecule of acetone- $d_6$ .



through  $\pi$ -coordination of one or both C=C bonds<sup>7a–f</sup> as well as the C=O bond<sup>7b,c</sup> or through coordination involving one or two oxygen lone pairs<sup>7c,e</sup> or the C $_{\beta}$  atom (which thus forms one or two metal–carbon bonds).<sup>7c,e–i</sup> In the latter case oxametallacycles may be formed.<sup>7c,e,i</sup> However, complexes of ruthenium with DBA derived directly from dibenzylideneacetone or its substituted analogues have not been reported.

## Results and Discussion

Reaction of  $Ru_3(CO)_{12}$  with DBA was carried out in boiling heptane. The course of the reaction was monitored by in situ IR spectra in the region of stretching vibrations of the coordinated carbonyl groups. After slow cooling, the reaction mixture was separated into a solution and a precipitate. From the solution, complexes **6** (17.1% yield) and **7** (3.5% yield) were isolated by column chromatography on silica gel. The precipitate contained complex **8** (8.2% yield) in the form of small yellow crystals (Scheme 2).

Yet another compound was isolated chromatographically from the reaction mixture. Its IR spectrum reveals no signals in the region of stretching vibrations of metal-coordinated carbonyl groups but a distinct absorption band due to stretching vibrations of the C=O bond ( $\nu(CO) = 1684$   $cm^{-1}$ ). Such a shift relative to the DBA molecule may be caused by hydrogenation of the CH=CH bonds. The  $^1H$  NMR data for this compound (see Table 1) are in a good agreement with the published

(7) (a) Cano, A. C.; Zuniga-Villarrreal, N.; Alvarez-Toledano, C.; Toscano, R. A.; Cervantes, M.; Daz, A.; Rudler, H. *J. Organomet. Chem.* **1994**, *464*, C23. (b) Bernes, S.; Toscano, R. A.; Cano, A. C.; Mellado, O. G.; Alvarez-Toledano, C.; Rudler, H.; Daran, J. C. *J. Organomet. Chem.* **1995**, *498*, 15. (c) Ortega-Jimenez, F.; Ortega-Alfaro, M. C.; Lopez-Cortes, J. P.; Toscano, R. A.; Velasco-Ibarra, L.; Pena-Cabrera, E.; Alvarez-Toledano, C. *Organometallics* **2000**, *19*, 4127. (d) Alvarez-Toledano, C.; Delgado, E.; Donnadiu, B.; Hernandez, E.; Martin, G.; Zamora, F. *Inorg. Chim. Acta* **2003**, *351*, 119. (e) Ros, J.; Solans, X.; Font-Altaba, M.; Mathieu, R. *Organometallics* **1984**, *3*, 1014. (f) Rivomanana, S.; Mongin, C.; Lavigne, G. *Organometallics* **1996**, *15*, 1195. (g) Knox, S. A. R.; Lloyd, B. R.; Morton, D. A. V.; Orpen, A. G.; Turner, M. L.; Hogarth, G. *Polyhedron* **1995**, *14*, 2723. (h) Fassler, N.; Huttner, G. *J. Organomet. Chem.* **1989**, *376*, 367. (i) Romero, A.; Vegas, A.; Dixneuf, P. H. *An. Quim.* **1996**, *92*, 299.



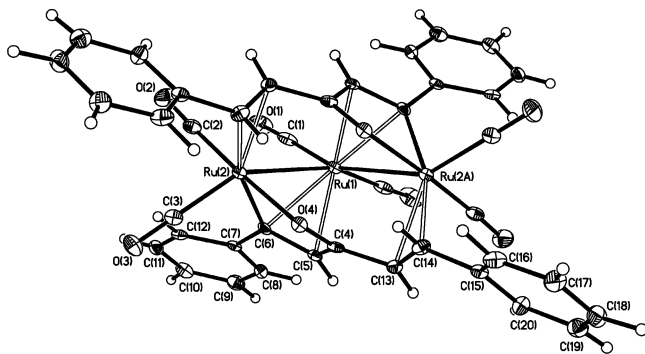


**Figure 1.** ORTEP representation (thermal ellipsoids drawn at the 30% probability level) of the molecular structure of complex **6**.

data for 1,5-diphenylpentan-3-one.<sup>8</sup> Upon formation of an oxaruthenacycle in reactions of  $\text{Ru}_3(\text{CO})_{12}$  with oxadienes, the ligand molecule loses a hydrogen atom, while an excess amount of the ligand acts as a hydrogen acceptor and thus undergoes reduction to the corresponding saturated ketone.<sup>2d</sup>

**Spectroscopic and X-ray Structural Characterization of 6.** The molecular structure of complex **6** was suggested on the basis of IR and NMR spectra (Table 1) and confirmed further by single-crystal X-ray diffraction analysis. The unique set of signals corresponding to the coordinated ligand was observed in the  $^1\text{H}$  NMR spectrum of **6**. Due to  $\pi$ -coordination of the double bond of the  $\text{PhCH}=\text{CH}$  group to the metal atom, the signals of olefin protons are considerably shifted to higher fields up to  $\delta$  4.36 and 4.65 ppm as compared to respective values of 7.08 and 7.74 ppm for the initial ligand. A decrease in the spin–spin coupling constant from 16.0 to 12.8 Hz also supports this conclusion. Similar values of the chemical shifts and spin–spin coupling constant ( $\delta$  4.78 and 5.29 ppm,  $^{\text{H}}\text{H}J = 11.3$  Hz) were reported for  $[\text{Fe}(\text{CO})_4]_2(\text{DBA})$ , where each of the two  $\text{Fe}(\text{CO})_4$  moieties is  $\pi$ -coordinated to one of the DBA  $\text{C}=\text{C}$  bonds.<sup>7a</sup> The signal of the  $\beta$ -carbon proton of oxaruthenacycle, which corresponds to the  $\text{C}=\text{C}$  bond  $\sigma,\pi$ -coordinated to two metal atoms, is observed at  $\delta$  5.35 ppm. For the closely related aforementioned complexes **2** and **3** containing  $\eta^3$ -coordinated oxaruthenacycles, the respective proton signals lie in the range  $\delta$  3–5 ppm. Only in one case were analogous proton signals attributed to the  $\sigma,\pi$ -coordinated  $\text{C}=\text{C}$  bond observed beyond this range, i.e., at  $\delta$  5.06 and 5.17 ppm, which is caused probably by an additional coordination of the oxaruthenacycle to the second ruthenium atom through the oxygen lone pair.<sup>2a</sup> The larger shift in **6** can be explained by an influence of the adjacent  $\pi$ -coordinated olefin bond. Therefore, the  $^1\text{H}$  NMR spectrum suggests that complex **6** contains an  $\eta^3$ -coordinated oxaruthenacycle and a  $\pi$ -coordinated  $\text{PhCH}=\text{CH}$  group. With respect to the metal core, the organic ligand acts as a seven-electron donor. The IR spectrum of **6** reveals six absorption bands of different intensities in the region of metal-coordinated carbonyls.

To verify the molecular structure of **6**, an X-ray diffraction study of its single crystal has been accomplished (Figure 1, Table 2). According to X-ray data,

**Table 2.** Selected Bond Lengths (Å) and Angles (deg) for Complex **6**

Ru(1)–Ru(2)	2.8402(8)	O(1)–C(1)	1.132(6)
Ru(1)–C(1)	1.902(6)	O(2)–C(2)	1.140(6)
Ru(1)–C(5)	2.233(4)	O(3)–C(3)	1.138(6)
Ru(1)–C(6)	2.233(4)	O(4)–C(4)	1.300(5)
Ru(2)–C(2)	1.861(5)	C(4)–C(13)	1.456(6)
Ru(2)–C(3)	1.899(5)	C(4)–C(5)	1.458(6)
Ru(2)–C(6)	2.080(5)	C(5)–C(6)	1.402(6)
Ru(2)–O(4)	2.087(3)	C(6)–C(7)	1.510(6)
Ru(2A) <sup>a</sup> –C(13)	2.268(5)	C(13)–C(14)	1.400(7)
Ru(2A) <sup>a</sup> –C(14)	2.352(5)	C(14)–C(15)	1.469(7)
Ru(2)–Ru(1)–Ru(2A) <sup>a</sup>	97.65(3)	C(13)–C(4)–C(5)	122.5(4)
C(6)–Ru(2)–O(4)	80.6(2)	C(6)–C(5)–C(4)	115.9(4)
C(4)–O(4)–Ru(2)	109.3(3)	C(5)–C(6)–C(7)	120.5(4)
O(1)–C(1)–Ru(1)	177.9(5)	C(5)–C(6)–Ru(2)	108.9(3)
O(2)–C(2)–Ru(2)	177.1(4)	C(7)–C(6)–Ru(2)	130.0(3)
O(3)–C(3)–Ru(2)	179.0(5)	C(14)–C(13)–C(4)	120.4(4)
O(4)–C(4)–C(13)	119.4(4)	C(13)–C(14)–C(15)	126.2(5)
O(4)–C(4)–C(5)	118.0(4)		

<sup>a</sup> Symmetry transformation  $-x, y, -z+3/2$  was used to generate equivalent atoms.

complex **6** is symmetric; in the unit cell it occupies a special position at the 2-fold axis passing through the Ru(1) atom. Two DBA molecules are coordinated to three ruthenium atoms. The open metal chain includes two Ru–Ru bonds with a bond length of 2.8402(8) Å, and the Ru(2)···Ru(2A) nonbonding distance is equal to 4.276 Å. Each ligand chelates one of the terminal ruthenium atoms forming the five-membered oxaruthenacycle. Two oxaruthenacycles are  $\eta^3$ -coordinated to the central ruthenium atom. The olefin bonds of each ligand that do not take part in chelation are  $\pi$ -coordinated to the ruthenium atoms at the opposite edges of the metal chain. Additionally, each ruthenium atom coordinates two carbonyl ligands. Taking into account  $\pi$ -coordination and metal–metal bonding, this results in a distorted octahedral ligand environment and completely filled 18-e shell for each ruthenium atom, so the EAN rule is fulfilled.

Additional coordination of the second olefin bond in **6** affects the geometry of the  $\eta^3$ -coordinated oxaruthenacycles insignificantly as compared to the studied earlier fragments in the bi- (**2**) and trinuclear (**3**) complexes.<sup>2a–c</sup> The molecular geometry of **6** is characterized by a slightly shortened endocyclic Ru–O bond (2.087(3) Å) and respectively an elongated C=O bond (1.300(5) Å) with respect to the corresponding mean values in **2** and **3** (2.12 and 1.28 Å, respectively). Most probably, this is due to the electron-donor influence of the  $\pi$ -coordinated olefin substituent at the keto group of the oxaruthenacycle. Furthermore, in contrast to the structures of **2** and **3**, complex **6** reveals symmetrical coordination of the Ru(1) atom to the metallacycle olefin bond (the Ru(1)–C(5) and Ru(1)–C(6) bond lengths are equalized to 2.233(4) Å), which probably reflects the contracting influence of an additional  $\pi$ -coordination of the exocyclic olefin bond. Meanwhile, coordination of the exocyclic olefin bond to the Ru(2) atom is asymmetric; the respective Ru(2)–C(13A) and Ru(2)–C(14A) bond lengths are 2.268(5) and 2.352(5) Å.

The five-membered oxaruthenacycle in **6** adopts a flattened twist conformation with the Ru(2) and O(4) atoms shifted up and down by 0.294 and 0.263 Å from the plane defined by the three carbon atoms. Due to coordination to the ruthenium atoms, the organic ligand

(8) Altava, B.; Burguete, M. I.; Garcia-Verdugo, E.; Luis, S. V.; Miravet, J. F.; Vicent, M. J. *Tetrahedron: Asymmetry* **2000**, *11*, 4885.

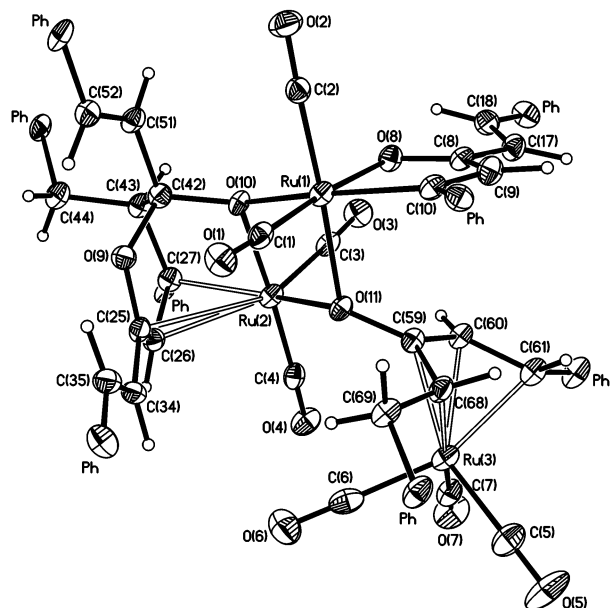


**Figure 2.** ORTEP representation (thermal ellipsoids drawn at the 30% probability level) of the molecular structure of complex **7**. Phenyl substitutions are omitted for clarity.

slightly deviates from planarity: the dihedral angle between the C(4)C(5)C(6) and C(4)C(13)C(14) planes is equal to 11.2°; the planes of the two phenyl substituents are rotated by 17.6° and 13.3° with respect to the corresponding three-carbon moieties.

**Spectroscopic and X-ray Structural Characterization of 7.** The second component of the solution obtained in the reaction of  $\text{Ru}_3(\text{CO})_{12}$  with DBA, i.e., complex **7**, has been characterized by IR and  $^1\text{H}$  NMR spectra; its molecular structure has been unequivocally determined by single-crystal X-ray diffraction analysis. According to X-ray data, complex **7** is composed of three Ru atoms linked together by four DBA ligands (Figure 2, Table 3). The oxadiene system of the first ligand chelates the Ru(1) atom, forming a five-membered oxaruthenacycle. Another two molecules of DBA are coupled with formation of a dihydropyran cycle, which is  $\eta^3$ -coordinated to the Ru(2) atom. The exocyclic oxygen atom (O(10)) of the dimerized ligand links the Ru(1) and Ru(2) atoms. Additionally, the Ru(1) and Ru(2) atoms are bridged by the enolate oxygen atom (O(11)) of the fourth ligand, which in turn is  $\eta^4$ -coordinated to the Ru(3) atom. The formed four-membered  $\text{Ru}_2\text{O}_2$  cycle is folded along the line connecting the Ru(1) and Ru(2) atoms by 17.1°. Each oxygen atom in this  $\text{Ru}_2\text{O}_2$  cycle acts as a three-electron donor and thus forms shorter covalent and longer coordination Ru–O bonds (Table 3).

The geometry of the five-membered oxaruthenacycle in **7** is similar to that observed earlier for uncoordinated oxaruthenacycles in chloride-bridged binuclear complexes  $\text{Ru}_2(\text{CO})_4(\mu\text{-Cl})_2[\text{O}=\text{C}(\text{R}')\text{-C}(\text{H})=\text{C}(\text{R}'')]_2$ , where  $\text{R}' = \text{Me}$ ,  $\text{R}'' = \text{Ph}$ ,<sup>2c</sup> or  $\text{R}' = \text{R}'' = \text{Fc}$ .<sup>2d</sup> This indicates that introduction of substituents into the chain of the starting oxadiene has only an insignificant influence on the geometry of the oxaruthenacycles. In contrast to the  $\eta^3$ -coordinated oxaruthenacycle in complex **6**, the uncoordinated oxaruthenacycle in **7** is planar (the Ru(1) and O(8) atoms are shifted by 0.089 and 0.088 Å up and

**Table 3.** Selected Bond Lengths (Å) and Angles (deg) for Complex **7**

Ru(1)–C(1)	1.865(6)	Ru(3)–C(60)	2.185(5)
Ru(1)–C(2)	1.844(6)	Ru(3)–C(61)	2.199(6)
Ru(1)–C(10)	2.039(5)	Ru(3)–C(68)	2.200(5)
Ru(1)–O(8)	2.087(4)	O(8)–C(8)	1.265(6)
Ru(1)–O(10)	2.154(3)	C(8)–C(9)	1.429(7)
Ru(1)–O(11)	2.147(3)	C(9)–C(10)	1.364(7)
Ru(2)–C(3)	1.838(6)	O(9)–C(25)	1.370(6)
Ru(2)–C(4)	1.853(6)	O(9)–C(42)	1.458(6)
Ru(2)–O(10)	2.056(3)	C(25)–C(26)	1.368(7)
Ru(2)–O(11)	2.217(3)	C(26)–C(27)	1.446(7)
Ru(2)–C(25)	2.717(5)	C(27)–C(43)	1.547(7)
Ru(2)–C(26)	2.274(5)	C(42)–C(43)	1.526(7)
Ru(2)–C(27)	2.118(5)	O(10)–C(42)	1.398(6)
Ru(3)–C(5)	1.916(7)	O(11)–C(59)	1.352(6)
Ru(3)–C(6)	1.896(7)	C(59)–C(60)	1.413(7)
Ru(3)–C(7)	1.921(6)	C(60)–C(68)	1.428(7)
Ru(3)–C(59)	2.249(5)	C(60)–C(61)	1.426(7)
O(11)–Ru(1)–O(10)	76.16(12)	C(25)–O(9)–C(42)	114.7(4)
O(10)–Ru(2)–O(11)	76.63(12)	C(26)–C(25)–O(9)	121.9(5)
Ru(2)–O(10)–Ru(1)	105.16(14)	C(25)–C(26)–C(27)	121.4(5)
Ru(1)–O(11)–Ru(2)	100.04(13)	C(26)–C(27)–C(43)	112.5(5)
C(10)–Ru(1)–O(8)	80.17(18)	O(9)–C(42)–C(43)	109.5(4)
C(8)–O(8)–Ru(1)	112.4(3)	C(42)–C(43)–C(27)	107.2(4)
O(8)–C(8)–C(9)	118.4(5)	C(60)–C(59)–C(68)	116.5(5)
C(10)–C(9)–C(8)	117.2(5)	C(59)–C(60)–C(61)	120.1(5)
C(9)–C(10)–Ru(1)	111.1(4)		

down from the plane defined by the three carbon atoms), while the C–C bonds in the organic part of the metalacycle are essentially alternating. A slight shortening of the endocyclic Ru(1)–C(10) and C(8)–C(9) bonds (2.039(5) and 1.429(7) Å) as compared to those in **6** (2.079(5) and 1.457(6) Å) indicates that the uncoordinated oxaruthenacycle has a partial ruthenafuran (i.e.,  $\text{O-Ru}=\text{C}(\text{Ph})\text{-C}(\text{H})=\text{C}(\text{CH}=\text{CHPh})$ ) character.<sup>2d</sup>

The nonplanar six-membered dihydropyran cycle in **7** adopts a distorted twist conformation with the C(42) and C(43) atoms shifted by 0.406 and 0.335 Å up and down from the mean plane defined by the four atoms O(9), C(25), C(26), and C(27) (which are planar to within 0.045 Å). A distinctive feature of coordination of this ligand to the Ru(2) atom consists in the substantial nonequivalency of the Ru(2)–C<sub>allyl</sub> bond lengths. It may be explained by the asymmetric ligand environment of the ruthenium atom involved in coordination. Indeed, the carbonyl group C(3)O(3) and the coordinated O(11) atom, which possess substantially different electron-donating properties, are situated in the pseudo-*trans* positions to the allylic fragment. The nonequivalence of the Ru–C<sub>allyl</sub> distances and substantial difference in the C–C bond lengths within the allylic fragment (see Table 3) allow an alternative description of the coordination to the ruthenium atom. This implies formation of a Ru–C  $\sigma$ -bond (Ru(2)–C(27)) and noticeable weakening of the  $\eta^2$ -coordination of the C(25)=C(26) olefin bond. Note that similar  $\eta^3$ -coordination of the dihydropyran ring was revealed by us earlier for products of reactions of  $\text{Ru}_3(\text{CO})_{12}$  with oxadienes. In particular, binuclear complexes **5** have been characterized as one of the major reaction products.<sup>2d</sup>

A distinctive feature of the five-membered oxaruthenacycle and the  $\eta^3$ -coordinated dihydropyran cycle in complex **7** is the presence of free olefin groups uncoordinated to ruthenium atoms; that is, the DBA ligand behaves identically to alkyl- and aryl-substituted oxadienes studied earlier. However, the similarity cannot be extended further. The presence of the second olefin

group in DBA starts to play a role in coordination of the fourth ligand in complex **7**. Coordination of the keto-oxygen O(11) atom to the Ru(1) and Ru(2) atoms polarizes the C=O bond so that the enol form of the ligand (produced by migration of the C=C double bond) becomes more stable. As a result, the C(68)C(59)C(60)C(61) diene system  $\eta^4$ -coordinated to the Ru(3) atom is formed. The C(69) atom becomes  $sp^3$ -hybridized and, respectively, the C(59)–O(11) bond is elongated to 1.352(6) Å, which is typical for C( $sp^2$ )–O single bonds, 1.354 Å.<sup>9</sup> It is necessary to note that the diene system in **7** adopts the *s-cis* configuration. This coincides with behavior of acyclic conjugated dienes: upon formation of  $\eta^4$ -complexes with transition metals, the *s-cis* arrangement predominates over the *s-trans* geometry, independently of the preferred conformation adopted by the free ligand.<sup>10</sup>

The IR and <sup>1</sup>H NMR data for complex **7** are in agreement with results of X-ray diffraction analysis. The IR spectrum reveals seven absorption bands of different intensities in the region of metal-coordinated carbonyls (Table 1). In the <sup>1</sup>H NMR spectrum, a singlet at  $\delta_H$  5.85 ppm can be attributed to the allyl proton of the dihydropyran cycle. Earlier, signals of similar protons in two complexes containing dihydropyran cycles were observed in the higher-field region, viz., at 3.82 and 5.16 ppm.<sup>2d</sup> In the former case, the pseudo-*trans* position to the allyl fragment is occupied by a ligand other than CO. The low-field shift of the proton signal in complex **7** as compared with the latter mentioned case may be due to a benzylidene substituent.

The part of the spectrum attributable to the ligand  $\eta^4$ -coordinated to the Ru(3) atom is of particular note. Protons of the coordinated C(60)=C(61) double bond give rise to two doublets at 1.96 and 5.64 ppm ( $J_{H-H} = 7.2$  Hz), with the terminal proton at the C(61) atom most likely contributing to the high-field signal.<sup>11</sup> The proton attached to the C(68) atom gives a multiplet at 3.09–3.14 ppm due to the spin–spin interaction with protons of the adjacent C(69)H<sub>2</sub> group.

**X-ray Structural Characterization of Complex 8.** According to X-ray diffraction data, complex **8** consists of two equivalent binuclear fragments (the crystallographic inversion center lies at the middle of the Ru(1) and Ru(1A) atoms, see Figure 3 and Table 4). Four ruthenium atoms are joined together by four DBA molecules, forming a system of fused metallacycles of three different types. The central four-membered Ru<sub>2</sub>O<sub>2</sub> cycle is planar with nonequivalent Ru(1)–O(3) (2.095(5) Å) and Ru(1)–O(3A) (2.258(5) Å) bonds. The O(3) atom is involved in the five-membered oxaruthenacycle Ru(1)C(7)C(8)C(9)O(3), in which the C(7) atom is saturated and the C(8)=C(9) double bond is  $\pi$ -coordinated to the Ru(2) atom (the Ru(2)–C(8) and Ru(2)–C(9) bond lengths are substantially different, viz., 2.279(8) and 2.447(8) Å). The olefin bond migrates to the carbon atom of the keto group so that the C(9)–O(3) bond becomes a single one (1.338(9) Å). The observed redistribution of the bonding within the chain of the initial DBA molecule

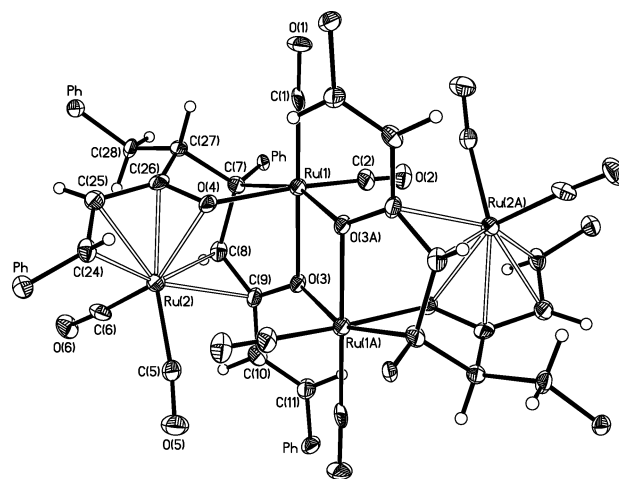


**Figure 3.** ORTEP representation (thermal ellipsoids drawn at the 30% probability level) of the molecular structure of complex **8**. Phenyl substitutions are omitted for clarity.

**Table 4.** Selected Bond Lengths (Å) and Angles (deg) for Complex **8**

Ru(1)–C(1)	1.853(9)	Ru(2)–C(25)	2.212(8)
Ru(1)–C(2)	1.854(11)	Ru(2)–C(26)	2.136(7)
Ru(1)–C(7)	2.098(8)	Ru(2)–O(4)	2.223(5)
Ru(1)–O(3)	2.094(5)	O(3)–C(9)	1.335(9)
Ru(1)–O(3A) <sup>a</sup>	2.259(5)	O(4)–C(26)	1.366(9)
Ru(1)–O(4)	2.116(5)	C(7)–C(8)	1.544(10)
Ru(2)–C(5)	1.940(9)	C(7)–C(27)	1.562(11)
Ru(2)–C(6)	1.822(9)	C(8)–C(9)	1.406(10)
Ru(2)–C(8)	2.276(8)	C(24)–C(25)	1.441(11)
Ru(2)–C(9)	2.444(8)	C(25)–C(26)	1.429(11)
Ru(2)–C(24)	2.208(8)	C(26)–C(27)	1.527(11)
O(3)–Ru(1)–O(3A) <sup>a</sup>	78.5(2)	C(26)–C(25)–C(24)	116.6(7)
Ru(1)–O(3)–Ru(1A) <sup>a</sup>	101.5(2)	O(4)–C(26)–C(25)	115.7(7)
O(3)–Ru(1)–C(7)	84.7(2)	C(7)–Ru(1)–O(4)	77.0(3)
C(9)–O(3)–Ru(1)	111.4(4)	C(26)–O(4)–Ru(1)	113.0(5)
C(8)–C(7)–Ru(1)	102.8(5)	O(4)–C(26)–C(27)	116.5(7)
C(9)–C(8)–C(7)	119.3(7)	C(26)–C(27)–C(7)	101.7(6)
O(3)–C(9)–C(8)	118.7(7)	C(27)–C(7)–Ru(1)	105.7(5)

<sup>a</sup> Symmetry transformation  $-x+1, -y+1, -z+1$  was used to generate equivalent atoms.

occurs as a result of coupling of two DBA molecules and formation of a new C–C bond (C(7)–C(27) 1.558(11) Å). The coupled ligand forms one more five-membered oxaruthenacycle Ru(1)C(7)C(27)C(26)O(4), which contains two saturated carbon atoms (C(7) and C(27)) and a formally double C(26)=O(4) bond that is  $\pi$ -coordinated to the Ru(2) atom. Due to additional coordination of the O(4) atom to the Ru(1), the C(26)=O(4) bond is elongated to 1.364(9) Å, which exceeds the normal values of 1.306–1.320 Å for  $\pi$ -coordinated carbonyl groups.<sup>12,13</sup> The remaining olefin bond of the second DBA molecule is also  $\pi$ -coordinated to the Ru(2) atom, which makes it possible to describe this moiety of complex **8** as a  $\eta^4$ -coordinated oxadiene fragment. Bond lengths in the C(24)C(25)C(26)O(4) chain are equalized; thus the  $\pi$ -coordination to the Ru(2) atom is nearly symmetrical. It is important to note that  $\eta^4$ -coordination of the oxadiene ligand to the ruthenium atom that was observed in complex **8** is quite rare in contrast to the  $\eta^4$ -coordination of diene ligands, frequently encountered in  $\pi$ -complexes

(9) Allen, F. H.; Kennard, O. K.; Watson, D. G.; Brammer, L.; Orpen, A. G.; Taylor, R. *J. Chem. Soc., Perkin Trans. 2* **1987**, S1.

(10) Erker, G.; Wicher, J.; Engel, K.; Rosenfeldt, F.; Dietrich, W. *J. Am. Chem. Soc.* **1980**, *102*, 6346.

(11) (a) Warren, J. D.; Clark, R. I. *Inorg. Chem.* **1970**, *9*, 373. (b) Ruh, S.; Philipsborn, W. *J. Organomet. Chem.* **1977**, *123*, C59.

(12) Hiraki, K.; Nonaka, A.; Matsunada, T.; Kawano, H. *J. Organomet. Chem.* **1999**, *574*, 121.

(13) Marcuzzi, A.; Linden, A.; Philipsborn, W. *Helv. Chim. Acta* **1993**, *76*, 976.



of transition metals. Probably, this is due to the fact that oxygen-containing ligands tend to coordinate ruthenium and osmium atoms via donation of lone pairs, forming chelate rings.<sup>14</sup> All  $\eta^4$ -enone complexes isolated so far are mononuclear and were obtained as a result of intramolecular rearrangement<sup>12,15</sup> or ligand-exchange reactions<sup>13</sup> rather than directly from the respective enones.

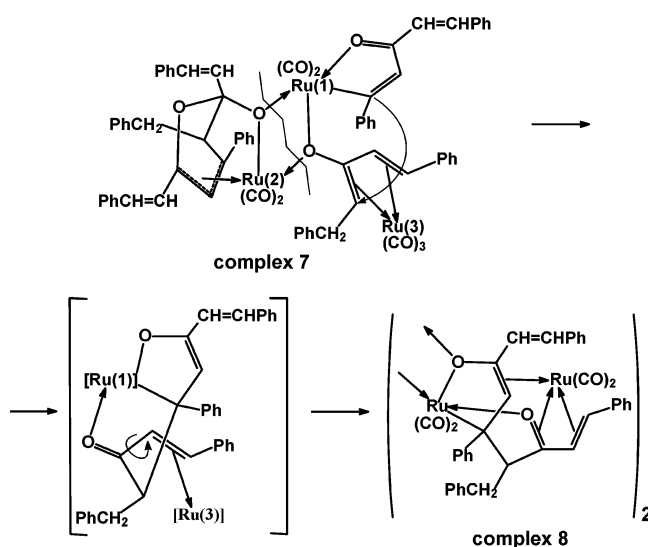
The structure of the five-membered oxaruthenacycles in **8** is noticeably different from the unsaturated oxaruthenacycles found in **6** and **7**. The Ru(1)C(7)C(8)C(9)O(3) cycle is nearly planar, adopting a conformation of a flattened envelope: the C(7) atom deviates from the plane of the other four cyclic atoms by 0.316 Å in the direction opposite the Ru(2) atom (the torsion angle C(8)C(9)O(3)Ru(1) is 0.5°). The Ru(1)–C(7) bond is elongated to 2.098(8) Å, as compared to 2.039(5) and 2.079(5) Å for similar bonds in the uncoordinated cycle in **7** and  $\eta^3$ -coordinated cycle in **6**. The Ru(1)–O(3) bond length of 2.095(5) Å is close to those of similar bonds in the oxaruthenacycles of complexes **6** and **7** (2.087(4) Å).

The nonplanar Ru(1)C(7)C(27)C(26)O(4) cycle in **8** adopts an envelope conformation: the C(7) atom deviates from the plane of the other four cyclic atoms by 0.844 Å in the direction of the Ru(2) atom (the torsion angle Ru(1)O(4)C(26)C(27) is 4.3°). The Ru(1)–O(4) bond is elongated to 2.117(5) Å.

The solid-state IR spectrum of complex **8** reveals four absorption bands of approximately equal intensities in the region of the coordinated carbonyls, which is in agreement with the symmetry of the molecule and the presence of two CO groups at each ruthenium atom in the *cis*-positions with respect to each other.

**Irreversible Transformation of 7 into 8.** The low yield of complex **7** in the thermal reaction of  $\text{Ru}_3(\text{CO})_{12}$  with DBA can indicate that this product is unstable and readily converts into other substances under the reaction conditions. To gain deeper insight into the transformation of complex **7**, an investigation of the chemical behavior of isolated complex **7** under the reaction conditions was carried out. We found that boiling **7** in heptane in the presence of DBA yields a mixture of products, from which complex **8** was isolated (see Experimental Section). It should be noted that no reaction occurs in the absence of DBA. On the other hand, complex **8** is also formed upon boiling **7** in heptane with benzylideneacetone (4-phenylbut-3-en-2-one, **1a**) instead of DBA. This suggests that complex **8** is formed as a result of the decomposition of complex **7** activated by additional DBA or another oxadiene (e.g., **1a**) molecule. We suppose that the decomposition of complex **7** goes through the cleavage of the longest Ru(2)–O(11) and Ru(1)–O(10) bonds (2.217(3), 2.154(3) Å) of the  $\text{Ru}_2\text{O}_2$  cycle. The reaction proceeds further as C–C intramolecular coupling of two ligands within the coordination sphere of the ruthenium atoms (see Scheme 3). The new C–C bond is formed between atoms C(10) and C(68). The distance between these two atoms in starting complex **7** (3.375(7) Å) is slightly shorter than the sum of the van der Waals radii of two carbon atoms,

Scheme 3



which probably facilitates coupling. As a result, the C(10) and C(68) atoms become  $\text{sp}^3$ -hybridized, and the order of the C(59)–O(11) bond increases, which enables involvement of the C=O bond in  $\pi$ -coordination to the Ru atom. Furthermore, the initial  $\eta^4$ -diene fragment transforms into the  $\eta^4$ -oxadiene in the resultant complex. The migration of the double bond from C(68)=C(59) to C(59)=O(11) is, probably, accompanied by a rotation around the C(59)–C(60) bond to realize the *cis*-arrangement of the C=C and C=O bonds, which is more favorable for coordination as in the case of butadienes.<sup>10</sup> Similar rearrangements within the coordination sphere of metal atoms were described for ruthenium complexes.<sup>16</sup> An additional driving force of the isomerization is, probably, formation of the stable chelating oxaruthenacycle.<sup>17</sup> Formation of complex **8** is completed by association of the two modified fragments of complex **7** through the Ru(1) and O(8) atoms to a symmetrical  $\text{Ru}_2\text{O}_2$  cycle. Complex **8** is insoluble in heptane and precipitates from the reaction mixture as crystalline powder (see Experimental Section), which prevents its further transformations under the reaction conditions.

It can be assumed that the second part of complex **7** (dihydropyran cycle and Ru(2) atom in Scheme 3) also undergoes coupling through the Ru(2) and O(10) atoms, yielding a compound similar to complex **5**.<sup>2a</sup> However, we failed to isolate this complex from the reaction mixture.

To our knowledge, only in one case was C–C coupling of oxadienes reported to date, viz., formation of the complex  $\text{Ru}_2(\text{CO})_5\{\mu\text{-}\eta^3\text{-}\eta^2\text{-CH}(\text{COOMe})\text{-C}(\text{COOMe})\text{-CH}(\text{COOMe})\text{-CH}(\text{COOMe})\}\{\eta^2\text{-CH}(\text{COOMe})\text{-CH}_2\text{-}(\text{COOMe})\}$  in the reaction of  $\text{Ru}_3(\text{CO})_{12}$  with dimethylfumarate.<sup>2f</sup> This complex is likely formed by introduction of an additional ligand molecule as in the case of the formation of the dihydropyran cycles.

**Solution Behavior of Complex 8 and X-ray Structural and Spectroscopic Characterization of Complex 9.** Complex **8** is poorly soluble in benzene. Other solvents (e.g.,  $\text{CHCl}_3$ ,  $\text{CH}_2\text{Cl}_2$ , ethers, acetonitrile, THF)

(14) Arce, A. J.; Sanetis, I. D.; Deeming, A. J.; Hardcastle, K. J.; Lee, R. *J. Organomet. Chem.* **1991**, *406*, 209.

(15) Jia, G.; Meek, D. W.; Gallucci, J. C. *Organometallics* **1990**, *9*, 2549.

(16) Blackmore, T.; Bruce, M. I.; Stone, F. G. A. *J. Chem. Soc., Dalton Trans.* **1974**, 106.

(17) Rybinskaya, M. I.; Krivikh, V. V. *Russ. Chem. Rev.* **1984**, *53*, 825 [*Uspehi Khim.* **1984**, *53*, 825].

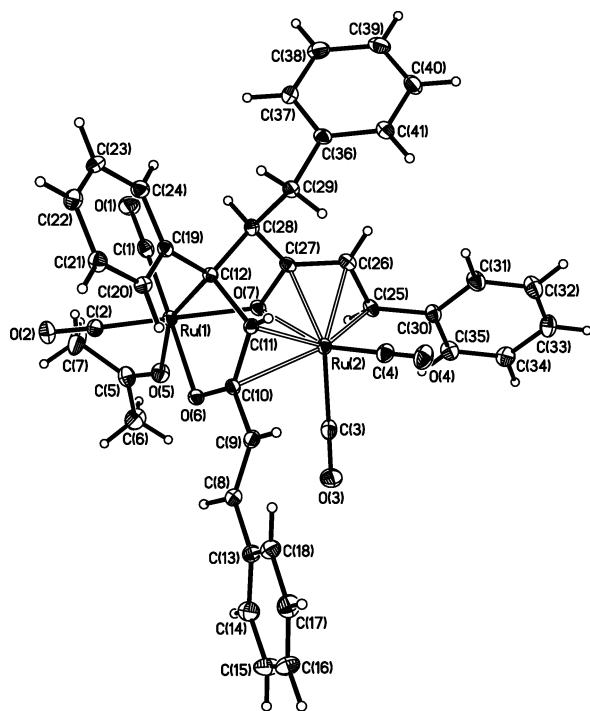


**Figure 4.** ORTEP representation (thermal ellipsoids drawn at the 30% probability level) of the molecular structure of complex **9**.

**Table 5. Selected Bond Lengths (Å) and Angles (deg) for Complex 9**

Ru(1)–C(1)	1.860(4)	Ru(2)–C(27)	2.122(3)
Ru(1)–C(2)	1.843(4)	Ru(2)–O(7)	2.174(2)
Ru(1)–C(12)	2.124(3)	O(5)–C(5)	1.238(5)
Ru(1)–O(5)	2.214(3)	O(6)–C(10)	1.301(4)
Ru(1)–O(6)	2.085(2)	O(7)–C(27)	1.365(4)
Ru(1)–O(7)	2.116(2)	C(10)–C(11)	1.414(5)
Ru(2)–C(3)	1.925(4)	C(11)–C(12)	1.546(5)
Ru(2)–C(4)	1.845(4)	C(12)–C(28)	1.546(5)
Ru(2)–C(10)	2.546(3)	C(25)–C(26)	1.430(5)
Ru(2)–C(11)	2.284(3)	C(26)–C(27)	1.393(5)
Ru(2)–C(25)	2.223(4)	C(27)–C(28)	1.517(5)
Ru(2)–C(26)	2.199(4)		
C(5)–O(5)–Ru(1)	136.6(3)	C(27)–O(7)–Ru(1)	113.6(2)
O(6)–Ru(1)–C(12)	84.3(1)	C(28)–C(12)–Ru(1)	104.6(2)
C(10)–O(6)–Ru(1)	110.9(2)	O(7)–C(27)–C(28)	115.5(3)
O(6)–C(10)–C(11)	121.0(3)	C(27)–C(28)–C(12)	102.8(3)
C(10)–C(11)–C(12)	116.8(3)	C(27)–C(26)–C(25)	117.7(3)
C(11)–C(12)–Ru(1)	101.7(2)	O(7)–C(27)–C(26)	115.7(3)
O(7)–Ru(1)–C(12)	76.6(1)	C(11)–C(12)–C(28)	108.2(3)

interact with the substance, leading to its chemical modification. Reversible changes occur with the complex upon dissolution in acetone, which is a weakly coordinating donor ligand. This made it possible to investigate solutions of complex **8** in more detail.

Upon dissolution of complex **8** in acetone, complex **9** is formed. In contrast to complex **8**, complex **9** is well soluble in hydrocarbons. Upon storage of hydrocarbon solutions of **9** for 1 day, the dissolved complex loses acetone, dimerizes, and converts into **8**, which precipitates as small crystals. To explore the changes occurring in the coordination sphere of the ruthenium atoms, we performed X-ray diffraction analysis of complex **9** (Figure 4, Table 5). As compared to the molecular structure of **8**, the central Ru<sub>2</sub>O<sub>2</sub> cycle in **9** is cleaved and the formed vacant coordination site is occupied by an acetone molecule. Therefore, complex **9** belongs to a small number of ruthenium complexes in which η<sup>1</sup>-

acetone is directly bonded to the metal center. The Ru(1)–O(5) bond length, 2.214(3) Å, lies within the normal range of 2.103–2.363 Å reported for similar species.<sup>18</sup> The presence of a donor acetone ligand strongly affects coordination of the C(12) atom situated in the *trans*-position. The Ru–C bond length increases from 2.098(8) Å in complex **8** up to 2.124(3) Å in **9**. Moreover, on going from **8** to **9**, the absence of additional coordination of the O(6) atom to the second ruthenium atom leads to noticeable shortening of the formally single C(10)–O(6) bond to 1.301(4) Å (as compared to 1.338(9) Å for the respective C(9)–O(3) bond in **8**). Other structural changes are insignificant.

In the vast majority of cases described in the literature, acetone occupies the free coordination site at the metal atom only in the absence of stronger coordinating agents, for example, in the course of rearrangements performed in acetone as a solvent.<sup>18b</sup> The ease of elimination of acetone was successfully exploited for deliberate modification of the complexes, e.g., for coordination of acetylenes or molecular nitrogen.<sup>18a</sup>

The IR spectrum of complex **9** reveals four bands in the region of stretching vibrations of metal-coordinated carbonyl groups, which are shifted to lower frequencies by 10 cm<sup>−1</sup>, on average, relative to the corresponding frequencies for complex **8** due to the electron-donating effect of the coordinated acetone ligand. The ν(C=O) band is observed at 1701 cm<sup>−1</sup>, which is close to the value observed for other ruthenium acetone complexes.<sup>18a</sup> Note that the value is smaller than the frequency typical for the free ligand appearing at 1710 cm<sup>−1</sup>, which is consistent with the decrease in the bonding order upon coordination.

The η<sup>4</sup>-oxadiene coordination of one of the ligands in **9** is strongly supported by the <sup>1</sup>H NMR spectrum. It is known that signals of the internal olefin protons for Fe(CO)<sub>3</sub>(η<sup>4</sup>-oxadiene) complexes are slightly shifted to higher field as compared with the respective uncoordinated ketones (Δδ is 0.5–1.0 ppm). Meanwhile, signals of the external protons have a significantly larger upfield shift (Δδ is 3.5–4.0 ppm).<sup>19</sup> In complex **9**, the η<sup>4</sup>-oxadiene system manifests itself as a doublet of doublets at δ 6.14 and 3.86 ppm (*J* = 8.9 Hz). In the <sup>1</sup>H NMR spectrum, signals of protons at the C(28) and C(29) atoms arise as three doublets of doublets at δ 5.06, 3.38, and 2.93 ppm. The presence of a chiral center at the C(28) atom results in the diastereotopy and hence inequivalency of protons at the C(29) atom. The lowest-field signal is attributed to the sp<sup>3</sup>-proton at the C(28) atom, in agreement with the <sup>1</sup>H NMR data for isomeric complexes Ru<sub>2</sub>(CO)<sub>4</sub>(η<sup>2</sup>-PhCOCH=CCOPh)<sub>2</sub>(μ-η<sup>2</sup>-η<sup>2</sup>-PhCOCHCHCOPh), in which signals of the protons lie in the range δ 5.30–5.70 ppm.<sup>2c</sup> The spin–spin coupling constant for the protons at the C(29) atom is <sup>2</sup>J<sub>H–H</sub> = 15.6 Hz, while the protons at C(29) are coupled with the proton at C(28) with <sup>3</sup>J<sub>H–H</sub> = 10.4 and 2.8 Hz.

(18) (a) Trimmel, G.; Slugovs, C.; Wiede, P.; Mereiter, K.; Sapunov, V. N.; Schmid, R.; Kirchner, K. *Inorg. Chem.* **1997**, *36*, 1076. (b) Esteruelas, M. A.; Lahoz, F. J.; Lopez, A. M.; Onate, E.; Oro, L. A. *Organometallics* **1994**, *13*, 1669.

(19) Nesmeyanov, A. N.; Shulpin, G. B.; Rybin, L. V.; Rybinskaya, M. I.; Gubenko, N. T.; Petrovskii, P. V.; Robas, B. I. *Zh. Obshch. Khim.* **1974**, *44*, 2032.



Table 6. Crystal Data, Data Collection, and Structure Refinement Parameters for 6–9

	6	7	8	9
formula	C <sub>40</sub> H <sub>26</sub> O <sub>8</sub> Ru <sub>3</sub> ·0.5(C <sub>6</sub> H <sub>14</sub> )	C <sub>75</sub> H <sub>56</sub> O <sub>11</sub> Ru <sub>3</sub>	C <sub>76</sub> H <sub>56</sub> O <sub>12</sub> Ru <sub>4</sub>	C <sub>41</sub> H <sub>34</sub> O <sub>7</sub> Ru <sub>2</sub> ·C <sub>3</sub> H <sub>6</sub> O
mol wt	980.90	1436.41	1565.49	898.90
cryst color, habit	yellow needle	red prism	yellow plate	yellow prism
cryst dimens, mm <sup>3</sup>	0.5 × 0.2 × 0.1	0.3 × 0.2 × 0.1	0.20 × 0.15 × 0.05	0.3 × 0.2 × 0.2
cryst syst	monoclinic	triclinic	triclinic	triclinic
space group	C2/c	P1	P1	P1
temperature, K	153(2)	110(2)	110(2)	110(2)
a, Å	14.120(4)	10.675(1)	10.496(2)	11.255(1)
b, Å	24.452(7)	12.942(2)	12.347(2)	14.146(2)
c, Å	11.080(3)	23.694(3)	12.762(2)	14.174(2)
α, deg		88.432(3)	75.860(3)	65.566(2)
β, deg	90.92(2)	83.478(3)	83.084(3)	80.367(2)
γ, deg		73.940(4)	76.385(3)	70.567(2)
V, Å <sup>3</sup>	3825(2)	3125.1(7)	1555.2(4)	1936.4(4)
Z	4	2	1	2
d <sub>calc</sub> , g/cm <sup>3</sup>	1.703	1.526	1.672	1.542
μ(Mo Kα λ = 0.71073 Å), cm <sup>-1</sup>	12.23	7.79	10.20	8.34
diffractometer	Syntex P2 <sub>1</sub>	SMART CCD 1000	SMART CCD 1000	SMART CCD 1000
2θ <sub>max</sub> , deg	50	56	44	60
range h, k, l	0 ≤ h ≤ 16, -3 ≤ k ≤ 29, -13 ≤ l ≤ 13	-14 ≤ h ≤ 14, -17 ≤ k ≤ 17, -31 ≤ l ≤ 31	-11 ≤ h ≤ 11, -12 ≤ k ≤ 13, -13 ≤ l ≤ 13	-15 ≤ h ≤ 15, -19 ≤ k ≤ 19, -19 ≤ l ≤ 19
reflectns collected	3512	30 794	9165	23 459
indep reflectns (R <sub>int</sub> )	3368 (0.0503)	14 876 (0.0532)	3837 (0.0618)	11 238 (0.0323)
obsd reflectns (I > 2σ(I))	2483	7052	2675	7767
R <sub>1</sub> (on F for obsd reflectns) <sup>a</sup>	0.0367	0.0597	0.0437	0.0514
wR <sub>2</sub> (on F <sup>2</sup> for all reflectns) <sup>b</sup>	0.0827	0.1187	0.1227	0.1225

$$^a R_1 = \sum ||F_o| - |F_c|| / \sum |F_o|. \quad ^b wR_2 = \{ \sum [w(F_o^2 - F_c^2)^2] / \sum w(F_o^2)^2 \}^{1/2}.$$

### Conclusion

According to the data obtained, formation of oxaruthenacycles may be regarded as the initial stage of the reaction of Ru<sub>3</sub>(CO)<sub>12</sub> with DBA. Further, the oxaruthenacycle interacts either with other ruthenium atoms, yielding complex **6**, or with another DBA molecule, yielding dihydropyran cycle and complex **7**. Complex **6** is stable and does not undergo any changes in the course of the reaction (see Experimental Section). The example of complex **6** clearly demonstrates that the presence of the second olefin bond in the ligand does not affect its ability to form an oxaruthenacycle. The vinyl substituent at the oxaruthenacycle represents simply an additional coordination site for metal atoms. In contrast with complex **6**, complex **7** is unstable and undergoes chemical transformations yielding other complexes. Therefore, it is impossible to isolate complex **7** with large yields irrespective of the reaction duration.

In complexes **7** and **8**, the presence of two C=C double bonds in DBA gives rise to the modification of the ligand due to C–C coupling and migration of the olefin bond. This leads to formation of the η<sup>4</sup>-diene (complex **7**) or η<sup>4</sup>-oxadiene (complex **8**) fragments.

The described complexes **6**, **7**, and **8** do not complete the thermal reaction of Ru<sub>3</sub>(CO)<sub>12</sub> with DBA. Two more complexes were isolated and characterized by IR spectroscopy (see Experimental Section), and as was mentioned above, formation of a compound similar to complex **5** is assumed. In the thermal reaction with Ru<sub>3</sub>(CO)<sub>12</sub>, the DBA ligand realizes the most its coordination abilities as an oxadiene system with an independent CH=CH substituent and displays peculiarities due to the presence of two olefin bonds linked in a conjugated system through the carbonyl group.

The large amount of products and their complicated separation and identification lead to a limited number of studies of reactions with organic ligands that have

several coordination centers. However, such investigations play a significant role in organometallic and organic chemistry because they assist with a more complete description of many chemical processes and transformations that occur with organic substrates in the presence of metal catalysts.

### Experimental Section

All reactions were carried out under an argon atmosphere using standard Schlenk techniques. Solvents were dried according to standard procedures. Column chromatography was performed with Aldrich silica gel (70–230 mesh). DBA was prepared by condensation of acetone and benzaldehyde.<sup>20</sup>

The <sup>1</sup>H NMR spectra were recorded on a Bruker AMX-400 spectrometer (400.13 MHz) in solutions of CDCl<sub>3</sub>, C<sub>6</sub>D<sub>6</sub> with trace signals of CHCl<sub>3</sub> (δ 7.25), and C<sub>6</sub>HD<sub>5</sub> (δ 7.25) as the internal standards, respectively. The IR spectra in solution were recorded on a Specord 75-IR spectrometer. The IR spectra in solid state were recorded on a Specord M82 spectrometer in Nujol.

**Reaction of Ru<sub>3</sub>(CO)<sub>12</sub> with DBA.** A mixture of Ru<sub>3</sub>(CO)<sub>12</sub> (320 mg, 0.5 mmol) and **1** (468.5 mg, 2 mmol) was refluxed in heptane (150 mL) for 4 h. After cooling to room temperature, the reaction mixture was filtered to separate the precipitate from solution. The filtrate was chromatographed on a column with silica gel. Elution with a 1:1 hexane/benzene mixture afforded complex **7** (25 mg, 3.5%), complex **6** (80 mg, 17.1%), and two other unidentified compounds with IR spectra for the first compound (18 mg) (ν(CO)/cm<sup>-1</sup>, hexane) 2044 s, 1980 s and for the second compound (trace amount) (ν(CO)/cm<sup>-1</sup>, hexane) 2092 s, 2042 s, 2034 w, 2008 s, 1990 w, 1950 sm, 1940 sm. Crystals of **6** (yellow needles) and **7** (red prisms) suitable for X-ray diffraction study were grown by slow evaporation of the hexane solutions. Mp: 198–202 °C (dec) for **6**. Anal. Found for **6** (%): C, 51.26; H, 2.85. Ru<sub>3</sub>C<sub>40</sub>H<sub>26</sub>O<sub>8</sub> Calcd (%): C, 51.23; H, 2.79. Mp: 207–210 °C (dec) for **7**. Anal. Found for **7** (%): C, 62.77; H, 4.22. Ru<sub>3</sub>C<sub>75</sub>H<sub>56</sub>O<sub>11</sub> Calcd (%): C, 62.70; H, 4.14. The precipitate flushed with benzene was composed of small

(20) Conard, C. R.; Dolliver, M. A. *Org. Synth. Coll.* **1943**, *2*, 167.

crystals of **8** (48 mg, 8.2%). Crystals of **8** (yellow plates) suitable for X-ray diffraction study were obtained by recrystallization from benzene. Mp: 220–225 °C (dec). Anal. Found (%): C, 58.25; H, 3.58. Ru<sub>2</sub>C<sub>38</sub>H<sub>28</sub>O<sub>6</sub> Calcd (%): C, 58.28; H, 3.70.

**Thermal Transformations of Complex 6.** A mixture of complex **6** (12.5 mg, 0.03 mmol) and **1** (17 mg, 0.075 mmol) in heptane (20 mL) was refluxed for 4 h. No changes in IR spectrum were detected.

**Thermal Transformations of Complex 7.** (a) A solution of complex **7** (53 mg, 0.037 mmol) in heptane was refluxed and monitored by IR spectroscopy. No spectral changes were detected after 3 h. (b) A mixture of complex **7** (53 mg, 0.037 mmol) and **1** (17 mg, 0.075 mmol) was refluxed in heptane (50 mL) for 2 h 30 min. The reaction was stopped when the IR signals of complex **7** disappeared. The solution contained a mixture of complexes with main IR signals ( $\nu(\text{CO})/\text{cm}^{-1}$ , hexane) 2044 s, 1980 s and precipitate. The reaction mixture was cooled to room temperature, and the precipitate was separated by filtering and flushed with benzene to afford small yellow crystals of complex **8** (6 mg, 13.8%). (c) A mixture of complex **7** (30 mg, 0.02 mmol) and 4-phenylbut-3-en-2-one (**1a**) (6 mg, 0.04 mmol) was refluxed in heptane (50 mL) for 2 h 30 min. The reaction was stopped when the IR signals of complex **7** disappeared. The solution contained a mixture of complexes and precipitate. The reaction mixture was cooled to room temperature, and the trace amount of precipitate was separated by filtering and flushed with benzene to afford small yellow crystals of complex **8**.

**Interaction of 8 with Acetone.** Complex **8** (16 mg, 0.01 mmol) in acetone (30 mL) was boiled until complete dissolution. The reaction mixture was cooled to room temperature and filtered. Yellow-gray crystals of **9** (12 mg, 69.8%) grew over the surface of the solution. Mp: 230–232 °C (dec). Anal. Found (%): C, 58.80; H, 4.49. Ru<sub>2</sub>C<sub>41</sub>H<sub>34</sub>O<sub>7</sub> Calcd (%): C, 58.57; H, 4.08.

**X-ray Diffraction Study.** Details of crystal data, data collection, and structure refinement of compounds **6–9** are presented in Table 6. The structures were solved by direct methods and refined by the full-matrix least-squares technique against  $F^2$  with anisotropic displacement parameters for non-hydrogen atoms. In the crystal structure of **6**, three additional peaks were located around an inversion center and 2-fold axis and proposed as a disordered solvate molecule of *n*-hexane with half-occupancy. In the crystal structure of **9**, a solvate molecule of acetone is present. Hydrogen atoms in complexes **6** and **9** were located from the Fourier synthesis and refined in the isotropic approximation; hydrogen atoms in the disordered solvate molecule of *n*-hexane in structure **6** are not defined. All hydrogen atoms in structures **7** and **8** were placed in calculated positions and refined in the riding model approximation. The SHELXTL-97<sup>21</sup> program package was used throughout the calculations.

**Acknowledgment.** We thank Dr. E. S. Shubina and co-workers for their technical assistance in measurements of IR spectra and fruitful discussion. The authors are also indebted to the Russian Foundation for Basic Research (Grant Nos. 04-03-32371 and 03-03-32499) for financial support.

**Supporting Information Available:** CIF files for the structures of **6–9**. This material is available free of charge via the Internet at <http://pubs.acs.org>.

OM0489958

(21) Sheldrick, G. M. *SHELXTL-97*, V5.10, Program for crystal structure refinement; Bruker AXS Inc.: Madison, WI 53719, 1997.